

## *Coordinated observation of local interstellar helium in the Heliosphere*

# Observations of the helium focusing cone with pickup ions

G. Gloeckler<sup>1,2</sup>, E. Möbius<sup>3</sup>, J. Geiss<sup>4</sup>, M. Bzowski<sup>5</sup>, S. Chalov<sup>6</sup>, H. Fahr<sup>7</sup>, D. R. McMullin<sup>8,\*</sup>, H. Noda<sup>9</sup>, M. Oka<sup>10</sup>, D. Ruciński<sup>5,\*\*</sup>, R. Skoug<sup>11</sup>, T. Terasawa<sup>9</sup>, R. von Steiger<sup>4</sup>, A. Yamazaki<sup>12</sup>, and T. Zurbuchen<sup>2</sup>

<sup>1</sup> Department of Physics and Institute for Physical Science and Technology, University of Maryland, College Park, MD 20742, USA

e-mail: gg10@umail.umd.edu

<sup>2</sup> Department of Atmospheric, Oceanic and Space Sciences, University of Michigan, Ann Arbor, MI 48109, USA

<sup>3</sup> Department of Physics and Space Science Center, University of New Hampshire, Durham, NH 03824, USA

<sup>4</sup> International Space Science Institute, Hallerstrasse 6, 3012 Bern, Switzerland

<sup>5</sup> Space Research Centre PAS, Bartycka 18A, 00-716 Warsaw, Poland

<sup>6</sup> Institute for Space Research, Moscow, Russia

<sup>7</sup> Institute of Astrophysics and Extraterrestrial Research, Bonn University, Auf dem Hügel 71, 53121 Bonn, Germany

<sup>8</sup> Space Sciences Center, University of Southern California, Los Angeles, CA 90089, USA

<sup>9</sup> National Astronomical Observatory of Japan, Hoshi-ga-oka 2-12, Misuzawa Iwate, Japan

<sup>10</sup> Department of Earth and Planetary Science, University of Tokyo, 7-3-1 Hongo, Bunkyo-ku, Tokyo 113-0033, Japan

<sup>11</sup> Los Alamos National Laboratory, Los Alamos, NM 87545, USA

<sup>12</sup> Communications Research Laboratory, Koganei, Tokyo 184-8795, Japan

Received 30 November 2003 / Accepted 30 January 2004

**Abstract.** The helium gravitational focusing cone has been observed using pickup He<sup>+</sup>, first during the solar minimum in 1984–1985 with the AMPTE/IRM spacecraft, and again in more detail from 1998 to 2002 with ACE and in 2000 with Nozomi. Five traversals of the cone allow us to obtain an accurate determination of the ecliptic longitude of the interstellar wind flow direction,  $\lambda = 74.43^\circ \pm 0.33^\circ$ , while observations of pickup He<sup>++</sup> with Ulysses give us an estimate, relatively free of instrumental systematic uncertainties, of the neutral He density,  $n_{\text{He}} = 0.0151 \pm 0.0015 \text{ cm}^{-3}$ , in the Local Interstellar Cloud. From best fits to the measured velocity distributions of pickup He<sup>+</sup> using time-stationary models we deduce the radial dependence and magnitude of electron-impact ionization rates that cannot presently be measured, and find this to be an important ionization process in the inner ( $\leq 0.5$  AU) heliosphere. We obtain excellent model fits to the 1998 cone profile using measured or deduced rates and known interstellar He parameters, and from this conclude that cross-field diffusion of pickup He<sup>+</sup> is small. Furthermore, we find no evidence for extra sources of He in or near the cone region. Best fits to the velocity distributions of He<sup>+</sup> are obtained assuming isotropic solar-wind-frame distributions, and we conclude from this that the scattering mean free path for pickup He<sup>+</sup> in the turbulent slow solar wind is small, probably less than 0.1 AU. We argue that application of 3D, time-dependent models for computation of the spatial distribution of interstellar neutral helium in the inner heliosphere may lead to excellent fits of short-term averaged pickup He<sup>+</sup> data without assuming loss rates that are significantly different from production rates.

**Key words.** ISM: abundances – plasmas – interplanetary medium

## 1. Introduction

The gravity of the Sun focuses interstellar heavy atoms that drift into the inner heliosphere due to the relative motion at  $\sim 26 \text{ km s}^{-1}$  of the Sun through the Local Interstellar Cloud (LIC), and concentrates them in roughly a conical region, called the gravitational focusing cone, in the direction opposite or downwind of the direction from which they arrive. Interstellar pickup ions are created by ionization of these atoms as they approach the Sun (Fahr 1973). Because He has the

smallest ionization probability (Ruciński et al. 1996, 1998) it is not significantly depleted even at 1 AU and He<sup>+</sup> is by far the most abundant interstellar pickup ion species at around 1 AU. Thus, the velocity distribution (phase space density spectrum) of pickup He<sup>+</sup> has its highest density and the helium pickup ion flux peaks in the downwind direction (Ruciński et al. 2003).

The helium focusing cone was first detected by EUV 58.4 nm backscattering observations of the neutral interstellar gas (Weller & Meier 1974) and interpreted in terms of the inflow gas kinematics by Fahr et al. (1978). Interstellar He<sup>+</sup> pickup ions were discovered in 1984 with the SULEICA instrument on the IRM spacecraft of the AMPTE mission (Möbius et al. 1985a; Hovestadt & Möbius 1988), which also made

\* Present address: Praxis, Inc., 2200 Mill Road, Alexandria, VA 22314, USA.

\*\* Deceased.

the first scan of the cone with particle measurements possible (Möbius et al. 1995). Almost 15 years later the characteristics of the helium cone could again be studied more thoroughly and systematically using a sensitive time-of-flight spectrometer on the ACE spacecraft in near Earth orbit at L1 (Gloeckler et al. 1998), and the Nozomi space probe to Mars (Yamamoto & Tsuruda 1998). Furthermore, simultaneous observations of the UV ionization rate of He are now available from the Solar EUV Monitor (SEM) in the CELIAS instrument package on SOHO (Hovestadt et al. 1995; Judge et al. 1997). Here we report in some detail on results of these investigations, concentrating on ACE and Ulysses measurements of pickup helium, the most comprehensive pickup He data set to date. The results provide an independent method to establish the interstellar neutral He distribution in the inner heliosphere. They are part of a concerted effort to derive the best current values for interstellar parameters (Möbius et al. 2004) from simultaneous observations of the neutral gas (Witte et al. 2004), pickup ions (this paper), and the EUV backscattering (Lallement et al. 2004; Vallergera et al. 2004).

A spacecraft such as ACE will traverse the helium focusing cone once every year with maximum pickup He flux observed around December 5 of each year. The shapes of the pickup He<sup>+</sup> spectra and the phase, maximum intensity, and time profiles of the pickup He<sup>+</sup> fluxes in the yearly focusing-cone peaks depend on the physical properties of He atoms in the LIC, such as their velocity relative to the Sun, number density and temperature, and on ionization processes in the heliosphere, which most likely have spatial and solar cycle variations (Ruciński et al. 2003). Pickup ion spectra may be used to constrain the radial density profiles of the parent atoms and thereby reveal ionization parameters that determine these profiles. However, before this can be done reliably, corrections for other effects that influence spectral shapes must be made.

## 2. Measurements of the He focusing cone

The first measurements of pickup He<sup>+</sup> in the helium focusing cone were made near the solar minimum in 1984 and 1985 with the SULEICA instrument (Möbius et al. 1985a; Hovestadt & Möbius 1988) on the AMPTE-IRM spacecraft (Häusler et al. 1985) orbiting the Earth. The SULEICA instrument (Möbius et al. 1985b) was among the new class of time-of-flight spectrometers developed at that time (see Gloeckler & Wenzel 2001) and was thus able to clearly identify He<sup>+</sup> ions. Figure 1a shows the observation of the He<sup>+</sup> flux during two consecutive crossings of the He focusing cone. Even though the IRM spacecraft spent a limited time in interplanetary space beyond the Earth's bow shock and data coverage was therefore limited, most of the He cone profile could be observed.

Observations of He<sup>+</sup> pickup ions at 1 AU were resumed again in early 1998 with the Solar Wind Ion Composition Spectrometer (SWICS) instrument (Gloeckler et al. 1998) on the ACE spacecraft. ACE orbits the Lagrangian L1 point about 200 earth radii upstream from Earth and is always in interplanetary space, thus providing nearly continuous coverage of interstellar He<sup>+</sup>. SWICS is an energy per charge time-of-flight spectrometer with post-acceleration and measures the mass/charge,

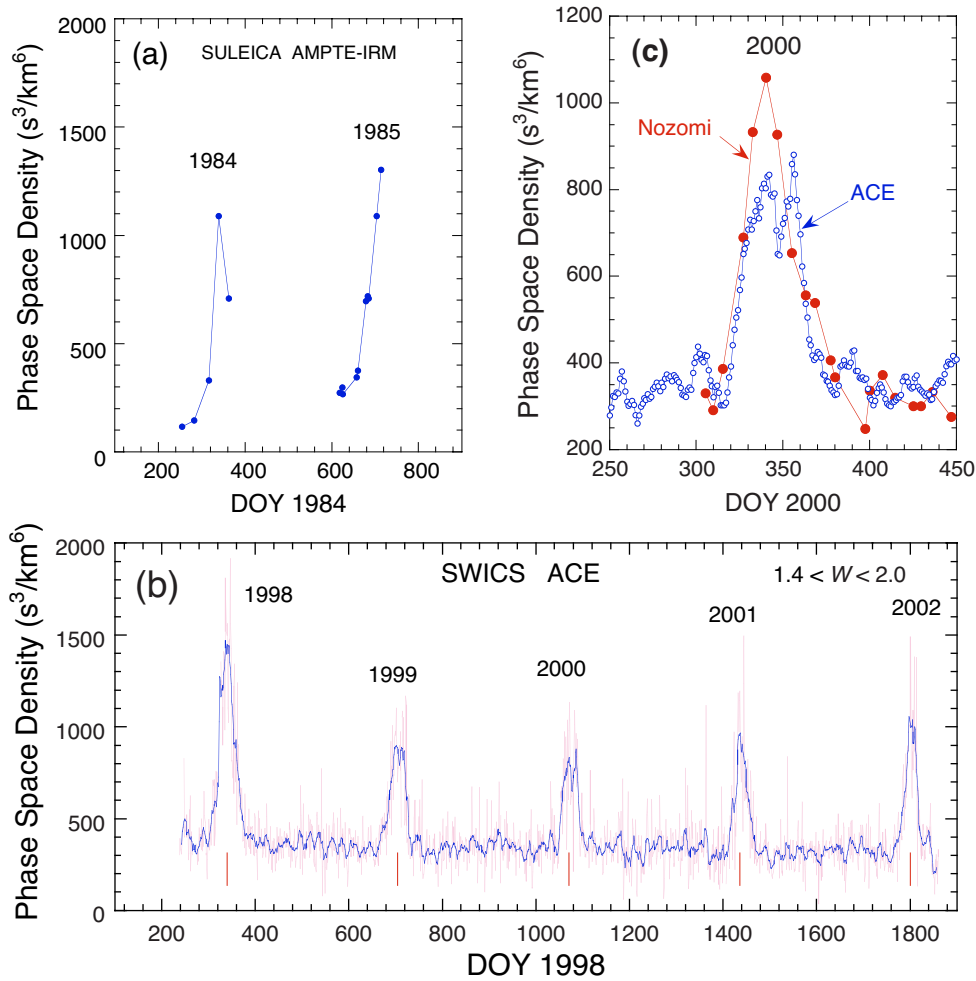
mass, speed and arrival direction of ions between  $\sim 0.6$  and  $\sim 100$  keV/charge. SWICS readily identifies He<sup>+</sup> ions and determines their velocity distribution or phase space density for normalized ion speeds  $W = V_{\text{ion}}/V_{\text{sw}}$  ( $V_{\text{ion}}$  is the ion speed and  $V_{\text{sw}}$  the solar wind speed) between  $\sim 0.9$  and  $\sim 5$ . Figure 1b shows the time variations of the phase space density of pickup He<sup>+</sup> measured with SWICS, averaged over  $1.4 \lesssim W \lesssim 2$ , which is approximately proportional to its flux. The 1-day averages (light violet curve) show large day-to-day variability. The 9-day running average (blue curve) reduces the variability and shows clearly the five He focusing cone traversals and the He density change with solar activity. The nature of the variability is not well understood, although several causes have been suggested (Gloeckler et al. 1994; Möbius et al. 1998; Schwadron et al. 1999; Gloeckler et al. 2001; Saul et al. 2003). Additional causes for these variations are also discussed in Sect. 8. The average density in the peaks of the cones and the density between cone crossings shows long-term changes, most likely due to solar cycle related variations in the ionization rates.

Figure 1c shows the 2000 helium gravitational focusing cone as seen by two spacecraft. The SWICS/ACE He<sup>+</sup> phase space density (open circles) is reproduced from Fig. 1b. The Nozomi measurements (Noda et al. 2001) of He<sup>+</sup> phase space density (solid circles), using a conventional energy per charge analyzer with excellent angular and energy resolution and low background noise, followed the first successful attempt to observe pickup He<sup>+</sup> on Geotail (Noda 2000; Oka et al. 2002) with a similar instrument. Careful analysis made it possible for the first time to observe pickup He without using a time-of-flight spectrometer. Both spacecraft crossed the cone at about the same time, but they did so at different radial distances from the Sun. Nozomi was about  $4 \times 10^6$  km further from the Sun than ACE. While the overall shape of the focusing cone as sampled at the two different locations is the same, different fine-structure is observed, which suggests that the density variations may be primarily spatial rather than temporal.

## 3. Interstellar parameters

The shape of the pickup He<sup>+</sup> focusing cone depends on He interstellar parameters that establish the spatial distribution of interstellar He atoms in the inner heliosphere, and on the ionization rates which are likely to have a spatial and time dependence. The only interstellar parameter that can be obtained reliably and independently from pickup helium measurements of the focusing cone profile is the ecliptic longitude,  $\lambda$ , of the interstellar wind flow direction. From the average of the positions of the peaks of the five He cone crossings (Fig. 1b) we obtain  $\lambda = 74.43^\circ \pm 0.33^\circ$ . This is in beautiful agreement with  $\lambda$  derived from direct measurements of neutral He with Ulysses (Witte et al. 2004) and from EUV backscattering observations with the EUVE satellite (Vallergera et al. 2004).

Measurements of the distribution function of pickup He<sup>+</sup> and He<sup>++</sup> also provide reliable and independent determinations of the density of interstellar He atoms, especially when made over long time periods at distances beyond  $\sim 5$  AU from the Sun. As described in some detail in Sect. 4, the best value for the interstellar neutral helium density near the termination



**Fig. 1.** Traversals of the gravitational focusing cone of interstellar helium at and near 1 AU for 1984, 1985, and 1998–2002, as observed with pickup ions. Shown is the phase space density of  $\text{He}^+$  pickup ions obtained with three different instruments. The observations with AMPTE SULEICA **a)** were made from Earth orbit, and with ACE SWICS **b), c)** from L1. The AMPTE observations were limited by the orbit, telemetry coverage and instrument sensitivity to high solar wind speeds only, thus not allowing any averaging over consecutive days. The cone position in longitude,  $\lambda = 74.6^\circ$  corresponds to DOY 339.75 (Earth crossing of the cone center). **c)** Observations of the 2000 cone with ACE and Nozomi. These observations are contiguous and have been averaged over 9 and 15 days, respectively. Nozomi is on an interplanetary trajectory just outside 1 AU. (See text for further explanation).

shock at  $\sim 100$  AU, obtained from the SWICS instrument on Ulysses using such observations, is  $n_{\text{He}} = 0.0151 \pm 0.0015 \text{ cm}^{-3}$ , which is again in good agreement with direct neutral He measurements from Ulysses (Witte et al. 2004). For the other interstellar parameters we use results obtained by the Interstellar Neutral Gas Experiment (GAS) (Witte et al. 1992) on Ulysses that directly measures the characteristics of interstellar He atoms in the heliosphere. The interstellar parameters we use in all of our model calculations are given in Table 1.

#### 4. Interstellar neutral He density determined from measurements and model calculations of the velocity distribution of pickup ions

The SWICS instruments on ACE and Ulysses (Gloeckler et al. 1998, 1992) provide observations of interstellar pickup ion distribution functions. SWICS on Ulysses as well as on ACE is an electrostatic deflection analyzer, time-of-flight spectrometer

**Table 1.** Interstellar neutral helium parameters.

Parameter	Unit	Value
Speed ( $V_o$ )	( $\text{km s}^{-1}$ )	26.3 <sup>a</sup>
Ecliptic Longitude ( $l$ )	( $^\circ$ )	74.4 <sup>b</sup>
Ecliptic Latitude ( $b$ )	( $^\circ$ )	-5.2 <sup>a</sup>
Temperature ( $T_o$ )	(K)	6300 <sup>a</sup>
Density ( $n_{\text{He}}$ )	( $\text{cm}^{-3}$ )	0.015 <sup>b</sup>

<sup>a</sup> Witte et al. (2004).

<sup>b</sup> Present work.

with post acceleration, and thus provides low-background measurements of the mass/charge ( $m/q$ ), mass ( $m$ ) and velocity ( $V_{\text{ion}}$ ) of ions. In each cycle of  $\sim 12$  min the analyzer is stepped through sixty-four logarithmically spaced

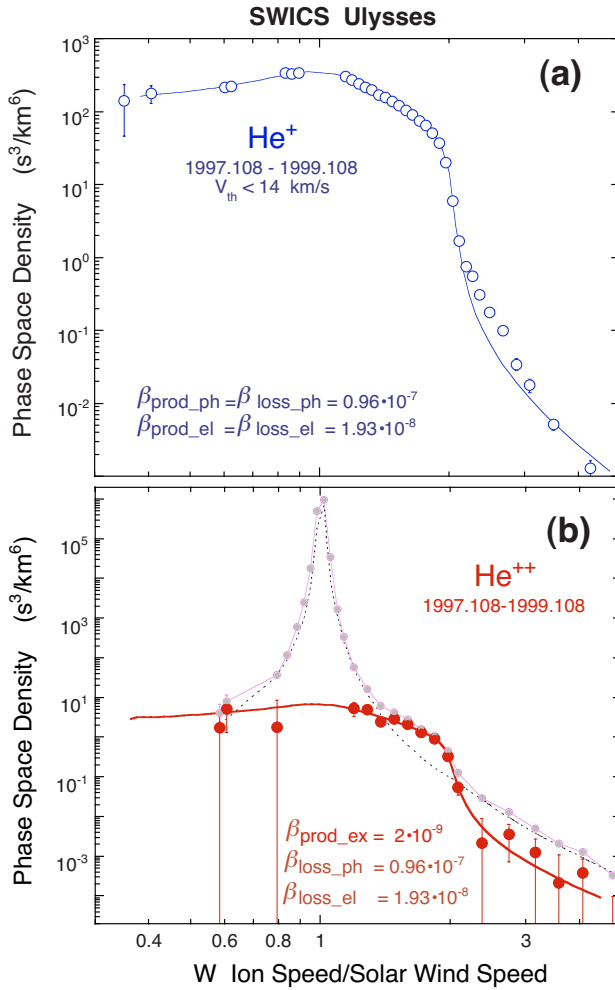


**Fig. 2.** Spacecraft-frame phase space density,  $F(W)$ , of pickup He<sup>+</sup> (upper panel, open circles) and He<sup>++</sup> (lower panel, solid circles) versus  $W$ , the ion speed divided by the solar wind He speed. Model curves are computed using ionization rates,  $\beta$ , given next to each model curve and interstellar parameters given in Table 1 (see text for more details). **a)** He<sup>+</sup> velocity spectrum showing the characteristic sharp cutoff near  $W = 2$ , and a suprathermal tail at higher speeds. The best fit requires a density  $n_{\text{He}} = 0.016 \text{ cm}^{-3}$  for neutral helium near the heliospheric termination shock at around 100 AU. **b)** Same as Fig. 2a except for He<sup>++</sup>. The pickup He<sup>++</sup> distribution (solid bold circles) was obtained from the measured total He<sup>++</sup> spectrum (solar wind plus pickup He<sup>++</sup>, solid faint circles) by subtracting from it the solar wind distribution (dotted curve) expressed as the sum of two kappa functions of the form  $F_{\text{sw}}(W) = 4.26 \times 10^5 \times [1 + \frac{1}{1.99} (\frac{W-1.004}{0.008})^2]^{-1.99} + 0.024 \times [1 + \frac{1}{0.8} (\frac{W-1.9}{0.5})^2]^{-0.8}$ . Pickup He<sup>++</sup> is produced predominantly by charge exchange with solar wind alpha particles. Using  $3.4 \times 10^{-16} \text{ cm}^2$  for the charge-exchange cross-section (Janev 1987) and the measured average solar wind alpha flux gives a production rate of  $2 \times 10^{-9} \text{ s}^{-1}$ . The best fit to the pickup He<sup>++</sup> spectrum is obtained with  $n_{\text{He}} = 0.0151 \text{ cm}^{-3}$ .

voltage steps, corresponding to ion energies between  $\sim 0.6$  and  $\sim 100 \text{ keV/charge}$ .

In Fig. 2 we plot the phase space density of He<sup>+</sup> (upper panel) and He<sup>++</sup> (lower panel) averaged over a two year period (1997 April 18 to 1999 April 18) as a function of  $W$ , the speed of helium ions divided by the simultaneously measured solar wind He speed,  $V_{\text{sw}}$ . During that time period Ulysses was

near the ecliptic (average latitude of  $-5.94^\circ$ ), near its aphe-  
 lion of 5.4 AU (average heliocentric distance of 5.26 AU) in  
 the slow solar wind (average speed of  $396 \text{ km s}^{-1}$ ) at cross-  
 wind ( $92^\circ$ ) to the inflow direction of the interstellar wind. To  
 minimize interference from solar wind alpha particles, espe-  
 cially in the case of He<sup>++</sup>, we excluded data for which solar  
 alpha particles had high thermal speed ( $\geq 14 \text{ km s}^{-1}$ ).

The distribution function,  $F(W)$  in the spacecraft-frame is  
 computed using  $F(W) = 378.4 \times (m/q)^2 \times (C/\epsilon^2)$ . Here  $F(W)$   
 is the phase space density in units of ( $\text{s}^3 \text{ km}^{-6}$ ),  $m/q$  is the ion  
 mass in units of  $\text{amu/e}$ ,  $\epsilon$  the energy per charge in  $\text{keV/e}$ , and  $C$   
 is the sector-averaged, efficiency-corrected counting rate of  
 ions in the appropriate  $m/q$  and mass ranges in counts/(12 s =  
 voltage step dwell time). The constant, 378.4, includes the  
 calculated instrument isotropic geometrical factor and unit con-  
 version factors. Energy-dependent efficiency curves were ob-  
 tained for He ions using preflight calibrations of the SWICS  
 instruments. The individual 12-min cycle spectra (raw counts  
 in the appropriate  $m/q$  and  $m$  ranges per  $\epsilon$  bin versus  $\log(\epsilon)$ )  
 were shifted in  $\log(\epsilon)$  to represent a distribution in  $\epsilon'$  that is  
 normalized so that the solar wind He peak is always at 2  $\text{keV/e}$ .  
 The measured ion speed divided by the solar wind speed,  $W$ , is  
 then equal to  $\{\epsilon'/(m/q)\}^{1/2}$ .

The measured distribution function of He<sup>+</sup>, shown in  
 Fig. 2a, has a sharp cutoff near  $W = 2$  and a suprathermal  
 tail. Data around  $W \approx 0.5$  and  $0.7$  (where mass information,  
 derived from the solid state detector energy measurement, and  
 thus triple coincidence analysis are not available) have been  
 excluded because of background contributions from solar wind  
 protons and alpha particles. The data gap around  $W \approx 1$  results  
 from removal of inner source (Geiss et al. 1995; Gloeckler &  
 Geiss 1998) He<sup>+</sup> that dominates in that portion of the spectrum.

The smooth curve is a model fit to the observed distribu-  
 tion. The model phase space density,  $F_m(W)$ , is obtained by  
 starting with the distribution function,  $f(R, W)$ , of a given ion  
 species in the solar wind frame, then applying a velocity trans-  
 formation to the spacecraft-frame coordinate system and inte-  
 grating this distribution over the instrument view angles to ob-  
 tain the predicted counting rate of that ion species,  $C_m$ , using  
 the directional geometrical factor of the instrument obtained in  
 preflight calibrations. Then, the model spacecraft-frame spec-  
 trum,  $F_m(W)$ , is computed from the predicted counting rate us-  
 ing  $F_m(W) = 378.4 \times (m/q)^2 \times (C_m/\epsilon^2)$ .

The model solar-wind-frame distribution function,  $f(R, w)$ ,  
 at radial distance  $R$  (AU) as a function of  $w = v_{\text{ion}}/v_{\text{max}}$   
 (where  $v_{\text{ion}}$  is the ion speed,  $v_{\text{max}}$  is the maximum ion speed  
 in the solar-wind-frame and is equal to  $V_{\text{sw}} - V_{\text{neutral}}(r)$ ,  $V_{\text{sw}}$   
 is the measured solar wind He speed, and  $V_{\text{neutral}}(r)$  is the  
 radial speed of neutrals at  $r = Rw^{3/\gamma}$ ) is calculated starting  
 with the generalized form of the Vasyliunas and Siscoe (1976)  
 equation for the case of strong pitch angle scattering, which, for  
 $w \leq 1$  is:

$$f(R, w) = \left[ \frac{3}{4\pi\gamma V_{\text{sw}} v_{\text{max}}^3} \right] \times n(r = Rw^{3/\gamma}) \times \left[ \frac{\beta_{\text{prod-ph}} \times w^{-3/2}}{R} + \frac{\beta_{\text{prod-el}} \times w^{3/\gamma-3}}{R\gamma^{-1}} \right]. \quad (1)$$

Here  $\gamma$  is the expansion factor ( $\gamma = 2$  for radial expansion,  $\gamma > 2$  for super-radial expansion), and  $\beta_{\text{prod-ph}}$  and  $\beta_{\text{prod-el}}$  are the production photo-ionization and electron-impact ionization rates respectively, at 1 AU. For  $w > 1$ ,  $f(R, w) = 0$ . The neutral helium density,  $n(r)$  at  $r = R w^{3/\gamma}$ , is computed using the hot model of Thomas (1978) with the “offset angle”,  $\theta$ , defined by  $\cos(\theta) = \mathbf{V}_o \cdot \mathbf{R} / (|\mathbf{V}_o| \times |\mathbf{R}|)$  and interstellar parameters given in Table 1. The vector  $\mathbf{V}_o$  is the velocity of the interstellar wind at a large heliocentric distance ( $\sim 100$  AU) and  $\mathbf{R}$  is the vector from the Sun to the point of observation (i.e. position of the spacecraft). Equation (1) incorporates the finite speed of neutrals at the time of their ionization, which has been demonstrated to have a significant effect on the pickup ion distribution by Möbius et al. (1999). It also allows for non-radial expansion ( $r^{-\gamma}$ , where  $\gamma = 2$  for radial expansion) of the solar wind. The neutral helium density profile as a function of  $r$  (radial distance from the Sun) depends on interstellar parameters (speed, density, and temperature of atomic helium near the termination shock), on the offset angle  $\theta$  (which requires knowledge of the inflow direction of the interstellar gas), on  $\mu$  (the ratio of radiation force to gravitational force), and on  $\beta_{\text{loss-ph}}$  and  $\beta_{\text{loss-el}}$  (the loss rates of neutral helium). In all of our model calculations of pickup He we use  $\mu = 0$ , interstellar parameters listed in Table 1, assume strictly radial expansion ( $\gamma = 2$ ) and isotropic solar wind frame distributions, implying small scattering mean free paths.

For very long-term averages, as is the case here, it is reasonable to assume that the loss rate of neutral helium,  $\beta_{\text{loss}}$ , is the same as the production rate,  $\beta_{\text{prod}}$ , of pickup  $\text{He}^+$ . We take  $\beta_{\text{loss}} = \beta_{\text{prod}} = \beta_{\text{ph}} + \beta_{\text{el}}$ , where  $\beta_{\text{ph}}$  is the average of the daily photo-ionization rate (at 1 AU) computed from the MgII line (McMullin et al. 2004) for the same two year period, and  $\beta_{\text{el}}$  is the electron-impact ionization rate whose magnitude and radial dependence were adjusted to fit the observed spectral shape.

In addition to the electron-impact ionization rate, the only other free parameter was the helium density near the termination shock,  $n_{\text{He}}$ , which was varied until the best fit to the data was obtained. In the model curve shown in Fig. 2a,  $n_{\text{He}} = 0.016 \text{ cm}^{-3}$  was used.

In Fig. 2b we display the measured particle velocity distribution function of  $\text{He}^{++}$  (solid faint circles). The pickup  $\text{He}^{++}$  distribution function (solid bold circles) is obtained by subtracting a typical kappa-function representation of the solar wind alpha spectrum (dotted curve) from the  $\text{He}^{++}$  distribution. Pickup  $\text{He}^{++}$  is produced predominantly by charge-exchange of neutral He with solar wind alpha particles (Ruciński et al. 1998), and while its density is only a few percent of the far more abundant  $\text{He}^+$ , its production rate is computed using the alpha-particle flux measured with the same instrument. Systematic uncertainties, especially in geometrical factors of instruments, are thus significantly reduced, and the phase space density of pickup  $\text{He}^{++}$ , as well as the density of neutral He near the termination shock derived from  $\text{He}^{++}$  pickup ion distributions, are more accurately determined.

The spectral shape of pickup  $\text{He}^{++}$  is similar to that of  $\text{He}^+$  (Fig. 2a) and the characteristic cutoff near  $W \approx 2$  is clearly visible, even in the combined spectrum (solid faint circles). The phase space density of pickup  $\text{He}^{++}$  ions with speeds  $W$

between  $\sim 1.5$  and  $\sim 2$  is well determined with small statistical uncertainty. Using the charge-exchange production rate,  $\beta_{\text{prod-ex}}$ , (product of the measured average solar wind alpha flux and charge-exchange cross-section) of  $2 \times 10^{-9} \text{ s}^{-1}$ , the best fit to the data is obtained with a neutral helium density near the termination shock,  $n_{\text{He}} = 0.0151 \pm 0.0015 \text{ cm}^{-3}$ . Most of the uncertainty results from systematic errors in the cross-section and poorly known minor contributions to the production of pickup  $\text{He}^{++}$  from other reactions. The fact that the best fit to the pickup  $\text{He}^+$  distribution function of Fig. 2a gave a somewhat higher value of  $0.016 \text{ cm}^{-3}$  is most likely due to a systematic uncertainty in the geometrical factor of the SWICS instrument on Ulysses. For all future model computations of pickup  $\text{He}^+$  distributions in this paper we will use  $n_{\text{He}} = 0.015 \text{ cm}^{-3}$ .

## 5. $\text{He}^+$ velocity distributions measured simultaneously in the crosswind direction at 1 and 5 AU

Data from nearly identical SWICS instruments on ACE and Ulysses allow us to determine the  $\text{He}^+$  distributions in the crosswind direction (offset angle  $\theta \approx 90^\circ$ ) at two different radial distances at the same time and thus gain essential information on ionization processes between 1 and  $\sim 5$  AU. This is illustrated in Fig. 3 that shows the 30-day averaged  $\text{He}^+$  spectrum measured by SWICS on ACE (top panel) at 1 AU and by SWICS on Ulysses (bottom panel) at 5.4 AU. Both ACE and Ulysses were at offset angle  $\theta$  of  $\sim 90^\circ$  near the ecliptic plane. Several spectral features are worth noticing when comparing the two spectra (see Fig. 3b where the  $\text{He}^+$  model distribution of Fig. 3a, divided by 2.4 is reproduced as the dashed curve). First, the observed phase space density at 1 AU is about a factor of 2.4 higher than at 5.4 AU. Second, the suprathermal tail is stronger at 5.4 compared to 1 AU. Third, the spectral shapes are different, showing the effects of ionization, in particular that due to electron-impact. Finally, at 1 AU the interstellar  $\text{He}^+$  pickup ion distribution cannot be measured below  $W \approx 1.17$  because of spill-over from the orders-of-magnitude larger solar wind proton and alpha particle fluxes, which in double-coincidence analysis where no mass determination can be made, completely dominates and obscures the interstellar  $\text{He}^+$  spectrum for  $W \lesssim 0.9$ . For  $W$  between  $\sim 0.9$  and  $\sim 1.17$ , inner source (Geiss et al. 1995; Gloeckler & Geiss 1998)  $\text{He}^+$  predominates.

The model curves are computed as described in Sect. 4 using equation (1), with  $\mu = 0$  and the interstellar He parameters listed in Table 1. To model the suprathermal tails of the distribution functions, each delta-function shell (i.e.  $f(R, w)$  at a given  $w$ ) is spread according to a kappa function distribution with spread parameters  $\sigma_t$  and  $\kappa_t$ . The photo-ionization production rates used were obtained from daily values at 1 AU measured by the SEM instrument on SOHO (McMullin et al. 2004) and averaged over the same time periods as the  $\text{He}^+$  spectra. The other 1-AU rates were adjusted to best fit the respective  $\text{He}^+$  velocity distributions. The radial dependence of the electron-impact ionization,  $\beta_{\text{el}}$ , is poorly known. However, because the exponent in the temperature law is found to vary with heliocentric distance from the Sun to the farthest distance

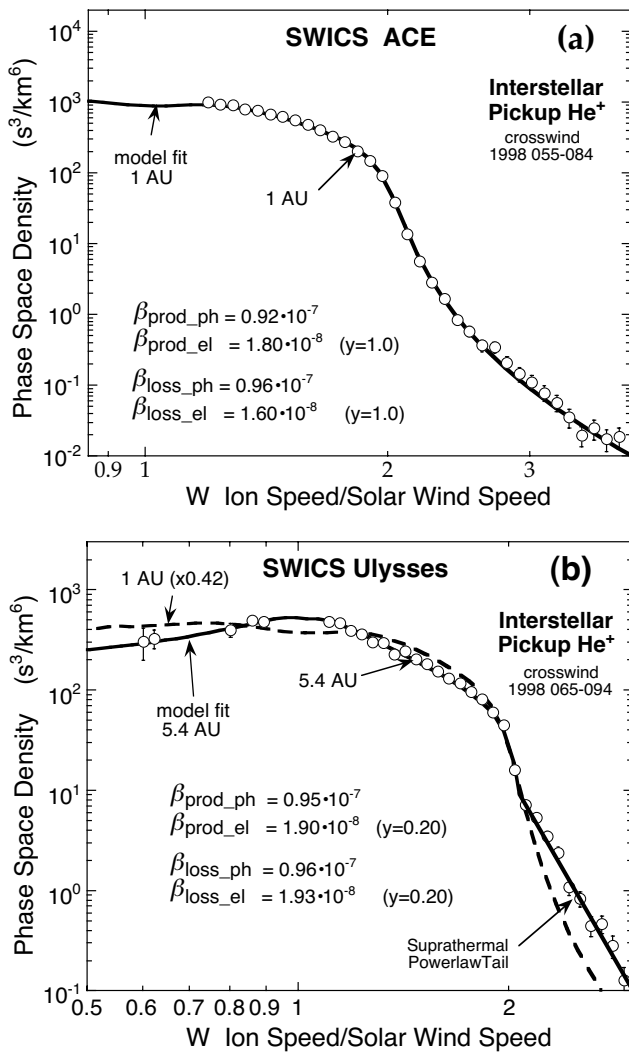


**Fig. 3.** Spacecraft-frame phase space density,  $F(W)$  of pickup  $\text{He}^+$  versus  $W$ , the ion speed divided by the solar wind  $\text{He}$  speed measured with SWICS on ACE at 1 AU (*upper panel*) and SWICS on Ulysses at 5.4 AU (*lower panel*) in the crosswind direction, each averaged over 30-day time periods indicated in the figure. The spectrum at 5.4 AU was averaged over a slightly different time period to account for propagation of pickup  $\text{He}^+$  from 1 to 5.4 AU. Model curves (solid curves) are computed using ionization rates,  $\beta$ , given next to each model curve, interstellar parameters given in Table 1, and kappa-function spread parameters,  $\sigma_i$  and  $\kappa_i$  of 0.025 and 2.0 for the 1 AU distribution, and 0.009 and 1.9 for the 5.4 AU spectrum, respectively (see text for more details). The tail on the  $\text{He}^+$  velocity distribution observed with Ulysses has, in addition, a steep power-law component of exponent  $\approx -9$ . Excellent fits to the data are obtained using nearly the same photo-ionization rates, but slightly different electron-impact rates. For purposes of comparing the spectral shapes at 1 and 5.4 AU, the 1 AU model curve, multiplied by 0.42, is reproduced as the dashed curve in the lower panel.

( $\sim 5$  AU) measured so far (Issautier et al. 1998),  $\beta_{\text{el}}$  is expected to have a radial dependence other than  $r^{-2}$  (see McMullin et al. (2004) and references therein for further discussion of electron-impact ionization rates). Here we use, for convenience, a simple power-law dependence of the form  $r^{-2.2}$  for  $\beta_{\text{el}}$  beyond

1 AU. It provides good fits to the observed  $\text{He}^+$  velocity distributions at both 1 and 5.4 AU and serves the purpose of this paper. For the radial dependence below 1 AU we used a linear combination of the  $\alpha = -1/3$  and  $\alpha = -2/3$  radial dependence of  $\beta_{\text{el}}$  of McMullin et al. (2004) where  $\alpha$  is the power-law exponent of the variation of the solar wind electron temperature with heliocentric radial distance  $r$ :

$$\beta_{\text{el}}(r) = (1 - y) \times g_{\frac{1}{3}}(r) + y \times g_{\frac{2}{3}}(r). \quad (2)$$

The numbers in parenthesis for the  $\beta_{\text{el}}$  in the figure give the mixing numbers,  $y$ , that provide the best fit to the data, where a value of  $y = 0$  indicates a purely  $\alpha = -1/3$  dependence and  $y = 1$  a purely  $\alpha = -2/3$  dependence. Typically, different values of  $\alpha$  are associated with different solar wind flows, such as fast and slow streams (Pilipp et al. 1987, 1990). We may conclude that excellent fits to the observed  $\text{He}^+$  distributions are possible both at 1 and 5.4 AU using measured ionization rates when available, and assuming reasonable values for the rates when direct measurements are lacking. Future work using measured solar wind electron spectra and  $\text{He}^+$  pickup ion distributions on ACE and Ulysses should allow us to further constrain the radial dependence of the electron-impact ionization rates inside 1 AU, where they are not measured at present, and study their time and spatial dependence.

## 6. $\text{He}^+$ velocity distributions in the focusing cone at 1 AU

The shapes of the velocity distributions of  $\text{He}^+$  measured by ACE are strongly affected by ionization processes at heliocentric distances below 1 AU. In the  $\text{He}$  gravitational focusing cone, where the neutral helium density changes by several factors, shorter time averages, typically of several days, are necessary to explore the structure of the cone. Figure 4 shows two sample spectra, each averaged over three days, one at the foot of the cone at offset angle  $\theta = 143^\circ$  (top panel) and the other at the peak of the cone ( $\theta = 173^\circ$ ). The model curves are again computed as before with interstellar parameters from Table 1,  $\mu = 0$  and production photo-ionization rates obtained from daily averages of the 1 AU SEM/SOHO data (McMullin et al. 2002). As before, we assumed an  $r^{-2.2}$  variation beyond 1 AU for the electron-impact ionization loss rate,  $\beta_{\text{loss-el}}$ . For the electron-impact production rate,  $\beta_{\text{prod-el}}$ , we used 3-day averages of the daily rates computed (McMullin et al. 2004) from solar wind electron spectra measured at 1 AU by the Solar Wind Electron Proton Alpha Monitor (McComas et al. 1998) on ACE.

As shown in Eq. (1), pickup  $\text{He}^+$  spectra measured at 1 AU depend on the radial profiles of the neutral helium density at less than 1 AU prevalent at that time. Although the spatial distribution of neutral helium is not directly measured, it can be calculated using assumed  $\text{He}$  loss rates. For electron-impact loss rates the radial dependence is again not measured directly and thus must be assumed. The simplest assumption is to take loss rates to be equal to the better known production rates. While this assumption seems to be valid for long-term ( $>30$ -day) averaged spectra measured outside the focusing cone (see Figs. 2 and 3), it does not produce acceptable

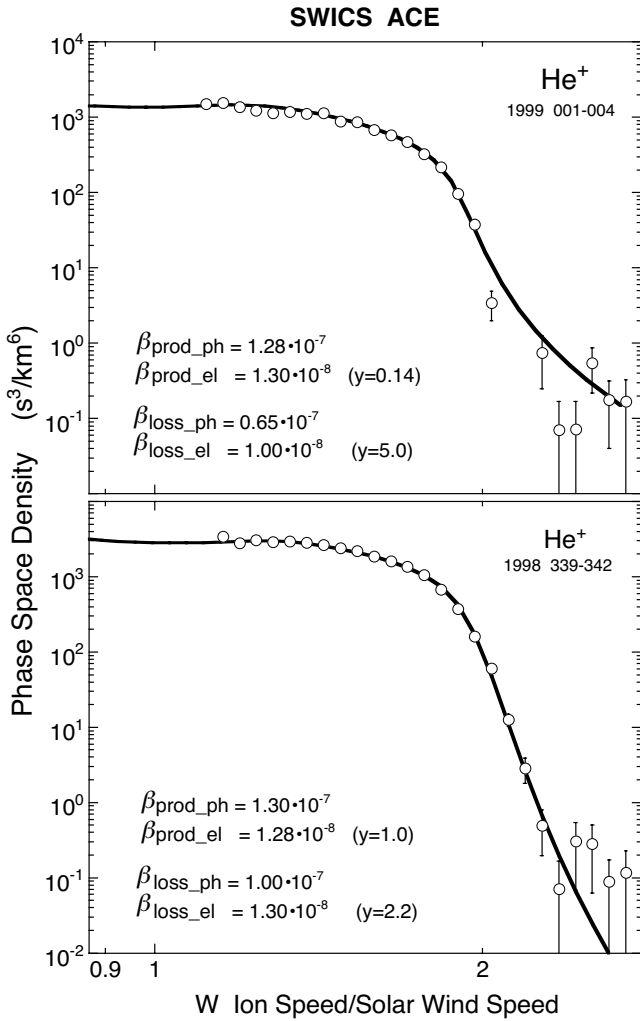


**Fig. 4.** Spacecraft-frame phase space density,  $F(W)$  of pickup  $\text{He}^+$  versus  $W$ , the ion speed divided by the solar wind  $\text{He}$  speed, measured with SWICS on ACE at 1 AU at the foot of the cone at offset angle  $\theta \approx 143^\circ$  (top panel), and at the peak of the cone at offset angle  $\theta \approx 173^\circ$  (lower panel). Each spectrum is averaged over a 3-day time period indicated in the figure. Model curves (solid curves) are computed using ionization rates,  $\beta$ , given next to each curve and interstellar parameters given in Table 1 (see text for more details). Excellent fits to the data are obtained using measured photo-ionization and electron-impact production rates, but much smaller photo-ionization loss rates. See text for further details.

fits to the 3-day averaged  $\text{He}^+$  distributions in the  $\text{He}$  focusing cone. The best fits to the measured spectra are obtained using respective loss rates listed in Fig. 4. Here again the value in parenthesis is  $y$ , the  $\beta_{\text{el}}$  mixing number defined in Eq. (2). We note here that values for  $y$  less than 0 and greater than 1 are possible.

The radial dependence of the electron-impact ionization rate,  $\beta_{\text{el}}$ , used to compute the model curves of Fig. 4 is shown in Fig. 5. Since all of the  $\beta_{\text{el}}$  curves, including the one corresponding to  $y = 0$  are found to fall off with distance  $r$  faster than  $r^{-2}$ , electron-impact ionization plays an important, if not a dominant, role in ionizing, and thus removing, neutral helium from the inner heliosphere ( $r \lesssim 0.3$  AU).

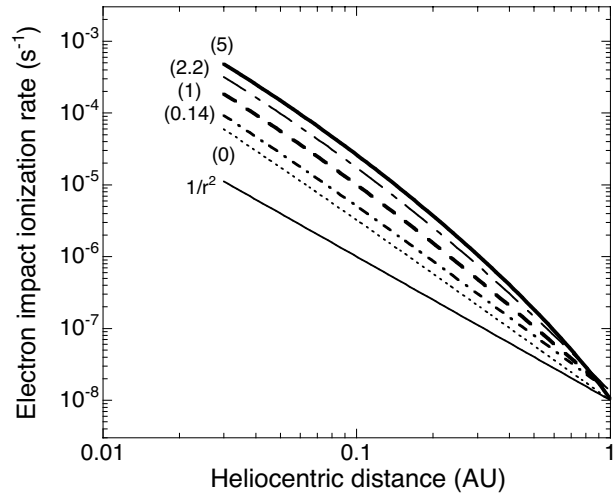


**Fig. 5.** Radial dependence of the electron-impact ionization rates used in Fig. 4. The solid line at the bottom is a pure  $r^{-2}$  dependence appropriate for photoionization rates. The value in parenthesis next to each curve is the mixing number,  $y$ , defined in Eq. (2). At 1 AU the values for all rates used are close to  $10^{-8} \text{ s}^{-1}$ . For computational simplicity we adopt a radial dependence proportional to  $r^{-2.2}$  beyond 1 AU. While the transition to an average  $r^{-2.2}$  dependence is likely to be gradual and not sudden as assumed here, this simplified approximation to the actual radial dependence of  $\beta_{\text{el}}$  is sufficient for the purpose of this paper.

The deduced photo-ionization loss rates that provide good fits to the data are lower than the corresponding measured photo-ionization production rates. These loss rates are more representative of solar minimum conditions that prevailed earlier, implying that the time-stationary models used here may be inadequate. Use of time-dependent models in the future could resolve these discrepancies. In addition, spectra averaged over relatively short time periods (days) may differ from the average due to the still partially unresolved substantial variations in the pickup ion fluxes and spectra.

The model curves very accurately reproduce the observed cutoff which in the solar wind frame should be at  $W_{\text{cutoff}} = 2 - V_{\text{neutral}}/V_{\text{sw}}$ , where  $V_{\text{neutral}}$  is the radial speed of neutrals computed using ballistic trajectories for zero-temperature neutral atoms under a purely gravitational force. While this may not be strictly valid because of the finite temperature of the interstellar gas, especially in the focusing cone, the excellent fits of the model curves around the cutoff of the measured velocity distributions justify this approximation.

## 7. Model fits to the 1998 focusing cone at 1 AU

In Fig. 6 are shown 3-point running averages of 3-day-averaged phase space densities averaged from 0.7 to 1.0 times  $W_{\text{cutoff}}$  from late 1998 to early 1999, along with model calculations averaged in the same fashion. Error bars take into account the accuracy in determining  $W_{\text{cutoff}}$ . To calculate the model curve we used values for  $\beta_{\text{prod}}$  measured at 1 AU. The electron-impact and photo-ionization loss rates as well as the mixing number,  $y$  that defines the radial dependence of  $\beta_{\text{el}}$  loss and

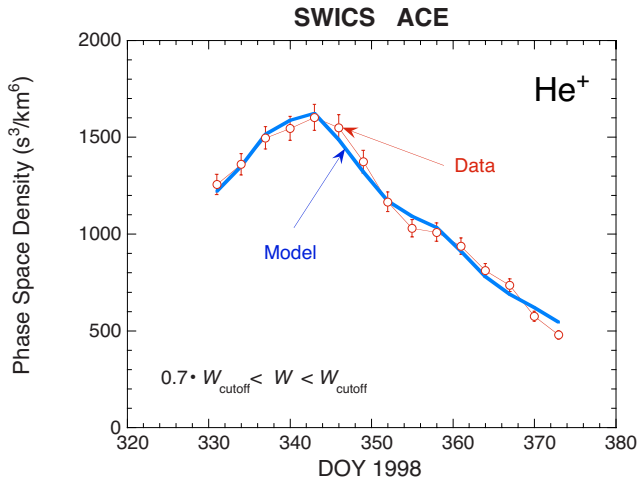


**Fig. 6.** Three-point running averages of 3-day-averaged phase space densities from 0.7 to 1.0 times  $W_{\text{cutoff}}$  from late 1998 to early 1999, and model calculations averaged in the same fashion. Error bars take into account the accuracy in determining  $W_{\text{cutoff}}$ . To calculate the model curve we used 3-day averages of daily values for  $\beta_{\text{prod}}$  computed from measured photon and solar wind electron spectra at 1 AU. For the radial dependence (mixing numbers) of the electron-impact loss and production rates and for the photo-ionization loss rates, we used values obtained from linear (in time) interpolations and extrapolations of the respective pairs of values listed next to the two model curves in Fig. 4.

production rates were obtained from linear (in time) interpolation or extrapolation using respective pairs of values that gave the best fits to the two 3-day averaged velocity spectra of Fig. 4. As discussed earlier, larger-than-expected electron-impact rates at  $<1$  AU, which cannot presently be measured, and near-solar-minimum values of photo-ionization loss rates were required to fit these spectra. The model curve provides an excellent fit to the data, indicating that cross-field diffusion of  $\text{He}^+$  pickup ions is relatively small, and that these pickup ions seem to faithfully map the neutral He gravitational focusing cone. It also implies that interstellar helium alone, without other low-speed neutral He sources, is sufficient to account for the pickup  $\text{He}^+$  measurements in the focusing cone of Fig. 6.

The average radial profiles of the neutral interstellar helium density,  $n_{\text{He}}(r, \theta)$ , during late 1998 deduced from pickup  $\text{He}^+$  observations are shown in Fig. 7 for offset angles  $173.2^\circ$  (downwind) and  $90^\circ$  (crosswind) respectively. It is interesting to note that the focusing cone neutral He ratio,  $n_{\text{He}}(r, 173.2^\circ)/n_{\text{He}}(r, 90^\circ)$ , reaches its maximum value of 5.7 at around 1 AU, in agreement with model predictions by Ruciński et al. (2003), thus making 1-AU observations of the focusing cone, as done with ACE, most sensitive for mapping the structure of the cone. Inside 1 AU the cone ratio diminishes with decreasing  $r$ , being approximately 2 at  $\sim 0.1$  AU ( $\sim 20$  solar radii). Below  $\sim 0.1$  AU it is not possible to obtain reliable estimates of  $n_{\text{He}}(r, \theta)$  from pickup  $\text{He}^+$  velocity distributions. We point out that because interstellar neutral He is negligibly affected by filtration (e.g. Gloeckler et al. 1997; Izmodenov et al. 2003), the He temperature in the interstellar medium has the same value as measured with the GAS instrument on Ulysses, and the calculated densities shown in Fig. 7 should also be valid

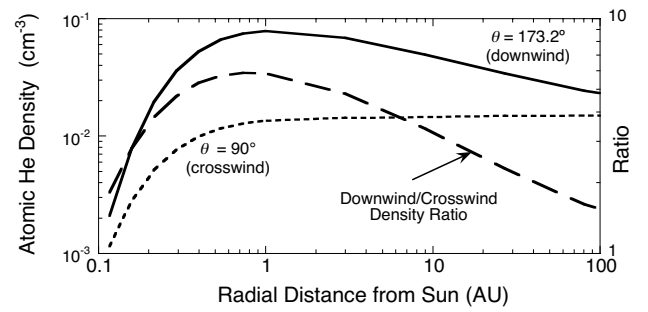


**Fig. 7.** Radial density profiles of interstellar neutral helium at offset angles  $\theta$  of  $90^\circ$  and  $173.2^\circ$  respectively, used to fit the  $\text{He}^+$  spectra of Fig. 3 and Fig. 4b respectively. The helium focusing cone is most pronounced around 1 AU. The dashed curve is the downwind ( $173.2^\circ$ ) to crosswind ( $90^\circ$ ) density ratio as a function of radial distance.

beyond the termination shock and heliopause most likely located at  $\sim 90$  AU and  $\sim 140$  AU respectively in the upstream direction (Izmodenov et al. 2003).

## 8. Summary and conclusions

The helium gravitational focusing cone is best studied in interplanetary space with a spacecraft such as ACE orbiting the Sun at 1 AU. Following the first observations of pickup  $\text{He}^+$  in the 1984 and 1985 helium cone (Möbius et al. 1985a; Hovestadt & Möbius 1988; Möbius et al. 1995), five crossings of the cone were measured with ACE (1998 to 2002) and one with the Nozomi spacecraft in 2000 (Yamamoto & Tsuruda 1998). The five cone traversals allowed us to find the ecliptic longitude of the inflow direction of the interstellar wind,  $\lambda = 74.43^\circ \pm 0.33^\circ$ , which agrees well with other independent determinations of this quantity (Witte et al. 2004; Lallement & Bertin 1992; Weller & Meier 1981; Lallement et al. 2004; Vallergera et al. 2004). This very close agreement of better than  $0.5^\circ$  appears somewhat surprising. Ruciński et al. (1993) had originally concluded that the position and width of the neutral gas cone structure remain preserved since it was believed that pickup ions were transported almost exactly radially, based on the widely held assumption that pitch-angle scattering for pickup ions was very efficient and the scattering mean free path small ( $\lesssim 0.1$  AU). However, Gloeckler et al. (1995) found that the pickup ion distributions during extended radial interplanetary magnetic field (IMF) conditions of the high-latitude, fast solar wind near solar minimum were highly anisotropic, which they attributed to a long mean free path ( $\sim 1$  AU) for pitch-angle scattering. This observation led Möbius et al. (1996) to suggest that the position of the cone observed with pickup ions may be shifted in longitude and its width increased. Möbius et al. (1996) concluded that the strength of these effects would be almost negligible for a mean free path of  $\sim 0.1$  AU, but quite substantial for values around  $\sim 1$  AU, and that the shift of the peak position should be strongest for an IMF direction of  $45^\circ$  and vanish for  $0^\circ$  and  $90^\circ$ . The fact that no significant shift in the position of the pickup  $\text{He}^+$  cone, nor a substantial increase in its width is observed, is most likely a consequence of a small ( $\sim 0.1$  AU) scattering mean free path in the in-ecliptic slow solar

wind near solar maximum where and when the present observations were made, as we discuss further below.

The overall cone profile as seen with pickup  $\text{He}^+$  as well as the  $\text{He}^+$  distribution functions are reasonably well understood, and can be properly modeled using a simple time-stationary hot model for the computation of the spatial distribution of neutral helium in the inner heliosphere and a generalized form of the isotropic Vasyliunas and Siscoe equation for the computation of pickup He ion spectra produced by ionization of neutral helium. The photo-ionization rate, which is most effective in ionizing helium at heliocentric distances greater than about 0.5 AU, is now well measured at 1 AU (McMullin et al. 2004). The electron-impact ionization rate is also measured with ACE at 1 AU and Ulysses from 1.4 to 5.4 AU over a wide range of latitudes. The radial dependence of the electron-impact ionization rate, however, is not well known, especially between  $\sim 0.1$  and 1 AU, where its contributions to the ionization of helium become quite significant. This radial dependence can fortunately be estimated from the spectral shapes of the  $\text{He}^+$  pickup ion velocity distributions. Thus, with knowledge of the temperature and relative velocity of interstellar He (Witte et al. 2004), and ionization rates directly measured or deduced from spectral shapes, it is possible to obtain good model fits to both the velocity distributions of pickup  $\text{He}^+$  and the He focusing cone profiles.

The interstellar neutral helium density in the Local Interstellar Cloud (LIC) can be independently obtained by combining measurements of pickup  $\text{He}^+$  and  $\text{He}^{++}$  in the cross-wind direction at  $\sim 5$  AU with SWICS on Ulysses. From the two-year averaged  $\text{He}^{++}$  spectrum we obtain a neutral helium density of  $0.0151 \pm 0.0015 \text{ cm}^{-3}$  in the LIC. This determination is free of systematic instrumental errors because both pickup  $\text{He}^{++}$  and the solar wind  $\text{He}^{++}$  flux that determines the production rate of pickup  $\text{He}^{++}$ , are measured by the same instrument. The quoted error in the measured He density is due mostly to the uncertainty in the cross-section for charge exchange between solar wind  $\text{He}^{++}$  and the neutral interstellar He (Janev 1987), which is by far the dominant process that produces these pickup ions, and to poor knowledge of cross-sections of other reactions which may produce a minor (less than 10%) fraction of pickup  $\text{He}^{++}$ .

While the average behavior of pickup He is basically well understood, some aspects such as the large variations in daily averages of the flux of  $\text{He}^+$  (light violet curve of Fig. 1b) are not. The cause or causes of the apparently random day-to-day variability are still a mystery with a number of possibilities proposed. Some of the variability may be due to small-scale spatial variations in the density of neutral helium and/or in the ionization rate, especially the electron-impact production rate, as suggested by comparison of the simultaneous observations of the 2000 He cone with ACE and Nozomi. The ionization rates are also most likely to vary with latitude and certainly with time on all scales. The radial dependence of the electron-impact rates could also be variable, affecting the shapes of the  $\text{He}^+$  distribution functions as suggested by our observations, and thus the flux. Among the other causes of the variability may be non-radial ( $r^{-\gamma}$ , where  $\gamma$  is smaller or larger than 2) expansions of the solar wind on various spatial scales.

Such non-radial expansions will introduce variations in the spectral shapes and hence the differential flux which is computed from these spectra. Finally, some of the observed variations may be due to the pickup process itself and the poorly known variations in the Alfvén speed, especially in the inner ( $\leq 0.5$  AU) heliosphere where these effects become important. These variations will again affect the spectral shapes and thus the  $\text{He}^+$  flux.

There are important conclusions we may draw from the results presented here. (1) Electron-impact ionization is important, especially close to the Sun ( $\leq 0.5$  AU). From the shapes of the pickup  $\text{He}^+$  spectra we can infer the average electron-impact ionization loss rates and their dependence on heliocentric distance. (2) Good model fits to the measured  $\text{He}^+$  flux profile (see Fig. 6) are possible using directly measured or inferred ionization rates and well established interstellar parameters. The ionization rates we infer from fits to measured spectral shapes of  $\text{He}^+$  are not unreasonable. This leads us to conclude that (a) large cross-field diffusion of pickup helium ions is not required to account for our observations, although a relatively small amount of cross-field diffusion through e.g. field line motion cannot be ruled out, and (b) no extra sources of neutral helium, in or outside the focusing cone, are evident in our data.

The observations presented here were made near solar maximum in the slow and more turbulent (compared to solar minimum) solar wind. We find consistently that the best fits to the measured distribution functions require isotropic distribution in the solar wind reference frame and hence small ( $< 0.1$  AU) scattering mean free paths. In fact, had we assumed anisotropic distributions associated with a large ( $\sim 1$  AU) scattering mean free path, as seen in the high-speed, high-latitude solar wind around solar minimum (Gloeckler 2003), unreasonably low values for the photo-ionization loss rates would have been required to obtain acceptable fits to the measured  $\text{He}^+$  distribution functions.

Finally, we stress the importance of time-dependent, 3D models (not available at present) to compute the spatial distribution of interstellar neutrals deep inside the inner heliosphere. Future use of such models to calculate distributions could resolve the remaining somewhat puzzling aspect in which present model fits applied to short-term averaged spectra ( $\sim 3$  days or less) require ionization loss rates significantly different from production rates.

*Acknowledgements.* The essential contributions of the many individuals at the Universities of Maryland and Bern, the Max-Planck-Institut für Aeronomie, and the Technical University of Braunschweig who contributed to the success of the SWICS experiments on Ulysses and ACE are most gratefully acknowledged. We thank Christine Gloeckler for her essential help with the ACE and Ulysses data reduction. This work was supported in part by NASA/Caltech grant NAG5-6912, NASA/JPL contract 955460, NASA SEC GI grant NAG5-10890 as well as by NSF grant ATM-9800781. M. Bz. and D. R. were supported by the Polish State Committee for Scientific Research grant 2P03C00519, while M. O. and T. T. were funded by Grant-in-Aids for Scientific Research from the MEXT, Japan. This work was initiated and partly carried out with support from the International Space Science Institute in the framework of an International Team entitled “Physical parameters of the LISM through coordinated observations of the gravitational focusing cone at 1 AU”.

## References

- Fahr, H. J. 1973, *Sol. Phys.*, 30, 193
- Fahr, H. J., Lay, G., & Wulf-Mathies, C. 1978, Derivation of interstellar helium gas parameters from an EUV-rocket observation, in *Space Research XVIII, Proc. of the Open Meetings of the Working Groups on Physical Sciences* (Oxford: Pergamon Press, Ltd.), 18, 393
- Geiss, J., Gloeckler, G., Fisk, L. A., & von Steiger, R. 1995, *J. Geophys. Res.*, 100, 23 373
- Gloeckler, G. 2003, Ubiquitous suprathermal tails on the solar wind and pickup ion distributions, in *Solar Wind Ten: Proc. of the Tenth International Solar Wind Conf., AIP Conf. Proc.*, ed. M. Velli, R. Bruno, & F. Malara (New York: AIP), 679, 583
- Gloeckler, G. & Geiss, J. 1998, *Space Sci. Rev.*, 86, 127
- Gloeckler, G., & Wenzel, K.-P. 2001, Acceleration processes of heliospheric particle populations, in *The Century of Space Science*, ed. J. Bleeker, J. Geiss, M. C. E. Huber, & A. Russo (Dordrecht: Kluwer Academic Publishers), 963
- Gloeckler, G., Geiss, J., Balsiger, H., et al. 1992, *A&AS*, 92, 267
- Gloeckler, G., Jokipii, J. R., Giacalone, J., & Geiss, J. 1994, *Geophys. Res. Lett.*, 21, 1565
- Gloeckler, G., Schwadron, N. A., Fisk, L. A., & Geiss, J. 1995, *Geophys. Res. Lett.*, 22, 2665
- Gloeckler, G., Fisk, L. A., & Geiss, J. 1997, *Nature*, 386, 374
- Gloeckler, G., Cain, J., Ipavich, F. M., et al. 1998, *Space Sci. Rev.*, 86, 497
- Gloeckler, G., Geiss, J., & Fisk, L. A. 2001, Heliospheric and interstellar phenomena revealed from observations of pickup ions, in *The Heliosphere near Solar Minimum: the Ulysses Perspectives*, ed. A. Balogh, E. J. Smith, & R. G. Marsden (Berlin: Springer-Praxis), 287
- Häusler, B., Melzner, F., Stöcker, J., et al. 1985, *IEEE Trans. on Geoscience and Remote Sensing*, GE-23, 192
- Hovestadt, D., & Möbius, E. 1988, Interstellar neutrals in interplanetary space, in *Cosmic abundances of matter; AIP Conf. Proc.*, ed. C. J. Waddington (New York: AIP), 183, 38
- Hovestadt, D., Hilchenbach, M., Bürgi, A., et al. 1995, *Sol. Phys.*, 162, 441
- Issautier, K., Meyer-Vernet, N., Moncuquet, M., & Hoang, S. 1998, *J. Geophys. Res.*, 103, 1969
- Izmodenov, V., Malama, Y., Gloeckler, G., & Geiss, J. 2003, *ApJ*, 594, L59
- Janev, R. K., Langer, W. D., Evans, K. Jr., & Post, D. E. Jr. 1987, *Elementary Processes in Hydrogen-Helium Plasmas*, in *Cross Sections and Reaction Rate Coefficients* (Berlin: Springer)
- Judge, D., McMullin, D. R., Ogawa, H. S., et al. 1997, *Sol. Phys.*, 177, 161
- Lallement, R., & Bertin, P. 1992, *A&A*, 266, 479
- Lallement, R., Raymond, J. C., Vallerga, J., et al. 2004, *A&A*, 426, 875
- McComas, D. J., Bame, S. J., Barker, P., et al. 1998, *Space Sci. Rev.*, 86, 563
- McMullin, D. R., Judge, D. L., Phillips, E., et al. 2002, Measuring the ionization rate of in-flowing interstellar helium with the SOHO/CELIAS/SEM, in *Proc. of the SOHO 11 Symposium on From Solar Min to Max: Half a Solar Cycle with SOHO*, ed. A. Wilson (Noordwijk: ESA) SP-508, 489
- McMullin, D., Pauluhn, A., Skoug, R., et al. 2004, *A&A*, 426, 885
- Möbius, E., Hovestadt, D., Klecker, B., et al. 1985, *Nature*, 318
- Möbius, E., Gloeckler, G., Hovestadt, D., et al. 1985, *IEEE Trans. on Geoscience and Remote Sensing*, GE-23, 274
- Möbius, E., Ruciński, D., Hovestadt, D., & Klecker, B. 1995, *A&A*, 304, 505
- Möbius, E., Ruciński, D., Isenberg, P. A., & Lee, M. A. 1996, *Ann. Geophys.*, 14, 492
- Möbius, E., Ruciński, D., Lee, M. A., & Isenberg, P. A. 1998, *J. Geophys. Res.*, 103, 257
- Möbius, E., Litvinenko, Y., Grünwaldt, H., et al. 1999, *Geophys. Res. Lett.*, 26, 3181
- Möbius, E., Bzowski, M., Chalov, S., et al. 2004, *A&A*, 426, 897
- Noda, H., Spacecraft observation of interstellar pickup He<sup>+</sup> by E/q type ion detectors, doctoral thesis, The University of Tokyo
- Noda, H., Terasawa, T., Saito, Y., et al. 2001, *Space Sci. Rev.*, 97, 423
- Oka, M., Terasawa, T., Noda, H., Saito, Y., & Mukai, T. 2002, *Geophys. Res. Lett.*, 29, 54
- Pilipp, W. G., Miggenrieder, H., Montgomery, M. D., et al. 1987, *J. Geophys. Res.*, 92, 1103
- Pilipp, W. G., Miggenrieder, H., Mühlhäuser, K.-H., Rosenbauer, H., & Schwenn, R. 1990, *J. Geophys. Res.*, 95, 6305
- Ruciński, D., Fahr, H. J., & Grzedziński, S. 1993, *Planet. Space Sci.*, 41, 773
- Ruciński, D., Cummings, A. C., Gloeckler, G., et al. 1996, *Space Sci. Rev.*, 78, 73
- Ruciński, D., Bzowski, M., & Fahr, H. J. 1998, *A&A*, 334, 337
- Ruciński, D., Bzowski, M., & Fahr, H. J. 2003, *Ann. Geophys.*, 21, 1315
- Schwadron, N. A., Zurbuchen, T. H., Fisk, L. A., & Gloeckler, G. 1999, *J. Geophys. Res.*, 104, 535
- Saul, L., Möbius, E., Litvinenko, Y., et al. 2003, SOHO CTOF Observations of Interstellar He<sup>+</sup> Pickup Ion Enhancements in Solar Wind Compression Region, in *Solar Wind Ten: Proc. of the Tenth International Solar Wind Conf., AIP Conf. Proc.*, ed. M. Velli, R. Bruno, & F. Malara (New York: AIP), 679, 778
- Thomas, G. E. 1978, *Ann. Rev. Earth Planet. Sci.*, 6, 173
- Vallerga, J., Lallement, R., Raymond, J., et al. 2004, *A&A*, 426, 855
- Vasyliunas, V. M., & Siscoe, G. L. 1976, *J. Geophys. Res.*, 81, 247
- Weller, C. S., & Meier, R. R. 1974, *ApJ*, 193, 471
- Weller, C. S., & Meier, R. R. 1981, *ApJ*, 246, 386
- Witte, M., Rosenbauer, H., Keppler, E., et al. 1992, *A&AS*, 92, 333
- Witte, M. 2004, *A&A*, 426, 835
- Yamamoto, T., & Tsuruda, K. 1998, *Earth, Planets & Space*, 50, 175